2020 IEEE/RSJ International Conference on Intelligent Robots and Systems (IROS)
October 25-29, 2020, Las Vegas, NV, USA (Virtual)

Development of Exo-Glove for Measuring 3-axis Forces Acting on the Human Finger without Obstructing Natural Human-Object Interaction

Prathamesh Sathe[1] Alexander Schmitz[1] Harris Kristanto[1]
Chincheng Hsu[1] Tito Pradhono Tomo[1] Sophon Somlor[1] and Sugano Shigeki[1]

Abstract— **Measuring the forces that humans exert with their fingers could have many potential applications, such as skill transfer from human experts to robots or monitoring humans. In this paper we introduce the "Exo-Glove" system, which can measure the joint angles and forces acting on the human finger without covering the skin that is in contact with the manipulated object. In particular, 3-axis sensors measure the deformation of the human skin on the sides of the finger to indirectly measure the 3-axis forces acting on the finger. To provide a frame of reference for the sensors, and to measure the joint angles of the human finger, an exoskeleton with remote center of motion (RCM) joints is used. Experiments showed that with the exoskeleton the quality of the force measurements can be improved.**

I. INTRODUCTION

Human experts have mastered various skills, most commonly using their hands. Transferring those skills to robots is not trivial. A direct way would be to measure the way that humans interact with their environment, which the robot could then try to reproduce. Measurements for the joint angles of the fingers and forces that the human hand exerts can be obtained from datagloves, but wearing gloves can make many tasks difficult for humans. Ideally, both the joint angles of the human hand and the interaction forces with the workpiece should be measured, without obstructing the human. Previously, we worked towards this goal by developing a wearable sensor for human fingertips [1]. It measures the 3-axis forces acting on the fingertip indirectly, by measuring the deformation of the fingertip pulp, and thereby achieves the goal of not obstructing the human, as the human can touch the workpiece directly with his skin. However, only the forces from the fingertip could be measured, and the joint angles could not be obtained. Moreover, mounting the sensor robustly to the fingertip was challenging, and there was no good frame of reference especially for measuring shear forces, i.e. the sensor tended to roll around the finger when the fingertip applied shear forces.

Therefore, in this paper, we not only apply the wearable sensor for the first time also to the other finger phalanges, but, moreover, we introduce an exoskeleton with RCM joints that provides a better frame of reference for shear force measurements. It also allows to measure the joint angles of the finger without placing the sensors directly at the joints.

This paper, like our previous work, focuses on forces that can be applied by only the finger, such as during fine manipulation or when grasping an object within the hand, not on the forces that can be produced by the wrist or arm when pushing an object. Principally, the fingerpad deformation, which is the basis for our sensor, saturates for higher forces, and therefore lends itself more to monitoring the forces during fine manipulation.

The rest of this paper is organized as follows. Section II reviews related work on wearable sensors. Section III describes the design of the Exo-Glove, i.e. the design of the wearable sensors for all finger phalanges as well as the exoskeleton with RCM joints. Section IV explains the procedure for calibrating as well as evaluating both the force and the joint angle sensors. Section V presents the results. Section VI draws conclusions and discusses possible future work.

II. RELATED WORKS

To the best of our knowledge, the idea of a wearable tactile force sensor was first presented by [2]. A one axis piezoresistive tactile sensor was wrapped around the fingertip. It covered the entire fingertip including the palmar side of the fingertip, which apparently is the most common contact area of the fingertip. A dome was designed to cover the top surface of the silicon islands in order to distribute the point load or pressure against the sensor. A major drawback of this approach was that it did not allow the person to experience the natural sense of touch while handling an object.

A small sized sensor based on the principle of photoplethysmography was introduced by [3] [4], and it was used to measure the force exerted by the fingertips. The sensor system consisted of several photodiodes and LEDs. When force was applied by the finger on an object the change in the color pattern of the fingernail was observed by the photodiodes that were mounted on top of the fingernail. Each of the three components of the force vector introduced to the fingertip resulted in a different coloration pattern. The initial research of this system produced significant error, which was improved in later research [5] [6] [7] [8]. While the sensor system provided 3-axis force measurements, the sensor system could only be utilized on the fingertip and could not be used for other finger phalanges.

Characteristics of the human fingertip pulp were highlighted in [9], by performing experiments with 20 subjects. The research concluded that the skin of the fingertip pulp

This research was supported by the JSPS Grant-in-Aid No. 19J14998, No. 19K14948, No. 19H02116, No. 19H01130, the Tateishi Science and Technology Foundation Research Grant (S), and the Research Institute for Science and Engineering, Waseda University.

[1]Prathamesh Sathe, Alexander Schmitz, Harris Kristanto, Chincheng Hsu, Tito Pradhono Tomo, Sophon Somlor and Shigeki Sugano are with Waseda University, Tokyo, Japan (corresponding author e-mail: sathe.prathamesh95@gmail.com)

stretches horizontally in response to vertical force acting on the palmar side of the fingertip. Furthermore, a structural model of the fingertip pulp was formulated when compressed by force [10]. The research concluded that the fingertip pulp structure has similar characteristics to a viscoelastic material in terms of hysteresis and nonlinear relation between the vertical external force and the vertical displacement of the fingertip. However, a limited amount of research has been done to analyze the deformation of the fingertip resulting from horizontal force [11]. The nonlinear finger flesh deformation was efficiently simulated in [12].

A finger tactile sensor based on finger pad deformation was introduced by [13]. One strain gauge was attached to each side of the clamp-like finger mounting to measure the horizontal expansion of the fingertip which can be converted to normal force. The sensor was mounted on a fingertip and enabled the user to directly touch the object without obstruction.

Using the same measuring principle based on finger pad deformation, [14] proposed a wearable device consisting of six photo-reflective sensors surrounding the fingertip. Three sensors facing down to the surface measured the distance to calculate the fingertip posture. The other three sensors facing the front and side of the fingertip measured the skin deformation which was then converted to 3-axis force. The paper stated that changes in the ambient light disturb the measurements.

A wearable vibration sensor was introduced by [15]. This sensor measured the vibration which is generated from the interaction between the fingertip and the object in the workspace. This device consisted of a flexible Polyvinylidene fluoride (PVDF) wrapped around the finger sensing the vibration from the fingertip. It was mounted between the distal interphalangeal joint (DIP) and proximal interphalangeal joint (PIP) to allow the fingertip to freely contact the object without obstruction. The sensor was capable of sensing the vibration propagated from the fingertip.

In [16], authors presented ThimbleSense, a wearable tactile force sensor which was embedded with force-torque sensors. An enhanced version of this sensor, the ExoSense, could measure in addition the fingertip position and orientation [17]. In both devices, the force-torque sensors were encapsulated within a cap-like structure which is meant to be worn on the finger while manipulating an object. Though this method could accurately measure forces while manipulating different objects, it did not promote natural interaction with the objects while manipulating them.

Bianchi et al. presented an integrated sensing glove which combined two sensing technologies to provide both hand posture sensing and tactile pressure sensing in a lightweight and stretchable device [18]. Only the pressure acting on the different parts of the hand, not the 3-axis force vectors could be measured. Furthermore, the hand was completely covered by the glove.

In summary, to the best of the authors knowledge, previously proposed finger tactile force sensors either obstruct the human haptic feedback, can be mounted only on the fingertip, or cannot measure 3-axis force.

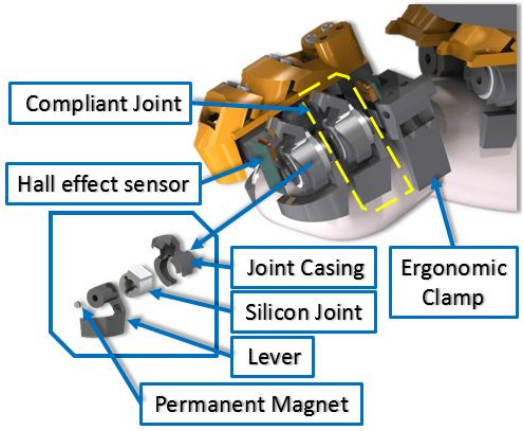

Fig. 1: Fingertip tactile Sensor

III. DESIGN OF EXO-GLOVE

The Exo-Glove consists of three 3-axis tactile sensor modules designed to be worn on the human finger. The sensors modules are supported by a Remote Center of Motion (RCM) mechanism which provides a mechanical frame of reference to the 3-axis tactile sensor modules. The mechanical joints of the Exo-Glove are embedded with Hall-effect based encoders to measure joint angles.

A. Tactile Sensor Modules for the Human Finger

This section briefly explains the tactile sensor modules for the human finger. The 3-axis tactile sensor modules are an integral part of the Exo-glove. The mechanical design of the sensor modules enables the user to wear it over the fingertip and the other finger segments (middle phalange and proximal phalange). The tactile sensor modules are designed to measure 3-axis force at the palmar side of the finger while performing a manipulation task. The mechanical design of the tactile sensors modules exposes the palmar side of the finger to allow unhindered interaction with the object while performing a manipulation task. This enables the user to feel the object thus, allowing the user to interact with the object naturally. The tactile sensor modules work on the principle of finger pad deformation which was introduced by [13]. A compliant joint mechanism was designed to conform to the changing deformation of the finger-pad while manipulating an object. The mechanism design will be explained briefly in the next section.

1) Fingertip Tactile Sensor Module: The fingertip tactile sensor based on distributed Hall-effect sensors has been presented previously in [1]. Fig. 1 illustrates the exploded view of the mechanical design of the fingertip tactile sensor module. The fingertip tactile sensor module is clamped to the DIP joint, where the skin is thin and the bone is thick, as shown in Fig.1. The fingertip tactile sensor uses four levers which conform to the deforming skin of the finger pad while manipulating an object. As each lever moves, its respective magnet moves relative to its 3-axis Hall-effect

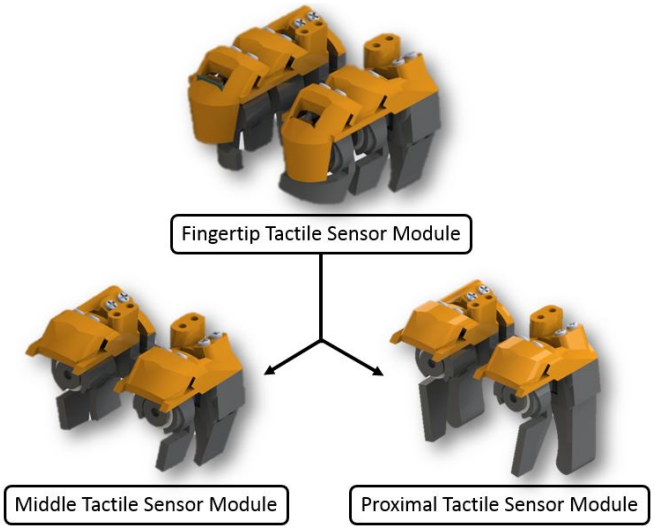

Fig. 2: Tactile Sensor Modules

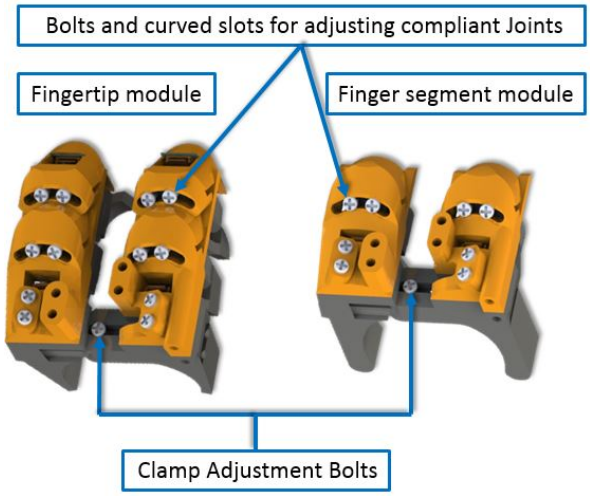

Fig. 3: Bolting for adjustment

sensor. Thereby, the deformation of the finger pulp can be measured, and indirectly (after calibration) the forces acting on the fingertip.

2) Finger Segment Tactile Sensor Modules: The mechanical design of the finger segment tactile sensor modules comprises of a clamping mechanism and a compliant lever mechanism, both derived largely from the fingertip tactile sensor module as shown in Fig. 2.

a) Clamping Mechanism: An ergonomic clamping mechanism was developed to clamp the sensors on the human finger. A bolt and slot arrangement as shown in the Fig. 3 was provided to change the size of the clamp in order to fit fingers of various shapes and sizes. The clamping mechanism of the middle phalange sensor module was designed to be clamped over the PIP joint. Whereas, the proximal phalange module was clamped to the middle of the proximal phalange. The clamp of the proximal phalange sensor module was curved at the bottom for ease of use and comfort as shown in Fig. 4.

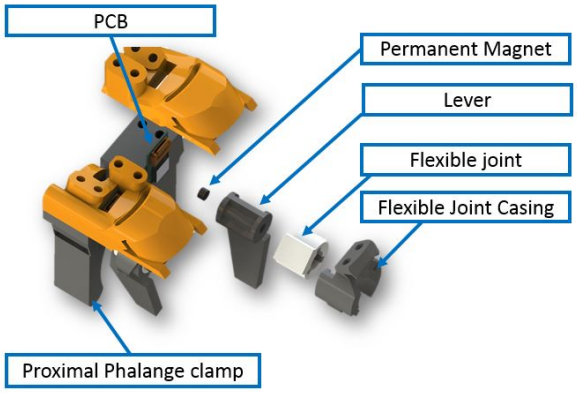

Fig. 4: Proximal Phalange Sensor Module

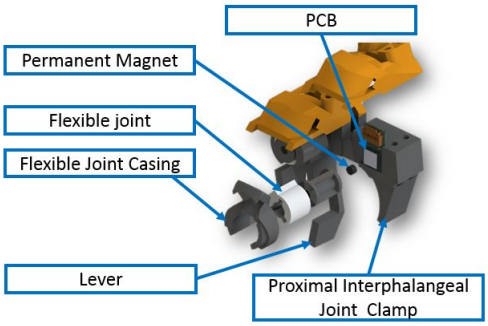

Fig. 5: Middle Phalange Sensor Module

b) Compliant Lever Mechanism: The compliant lever mechanism consists of a joint casing which houses a flexible joint. Due to the ease of manufacturing and compact structural requirement of the sensor module, the compliant joint was made from molded silicon (Dragon Skin 30 from Smooth-On). The silicon joint envelopes a lever which houses a permanent magnet such that its North pole faces the Hall-effect sensor as shown in the Fig. 1, 4 and 5. The entire mechanism behaves similar to a compliant ball and socket joint which enables the lever to move spatially in three axes. The levers are placed on either side of the finger for both the proximal and middle tactile sensor modules as shown in Fig. 2. Such compliance in the mechanical system enables the lever to conform to the changing shape of the finger pad while handling objects. Further, the orientation of the levers can be adjusted by tightening and loosening the bolts placed within the curved slots as shown in the Fig.3, thereby making the sensor modules able to adapt to various finger sizes. The three tactile sensor module prototypes were printed using SLA type Photon 3D Printers. SLA printing technology was chosen for smooth textured and high detailed prints.

3) Custom printed circuit boards (PCBs): A PCB as shown in Figs. 4 and 5 was used with dimensions 8.5mm

x 5mm. The PCB comprises of the MLX90393 chip, which is a 3-axis Hall-effect sensor from Melexis. All PCBs can be connected to one I2C bus via a compact FFC (Flexible Flat Cable) cable. The PCBs act as children to the microcontroller (Arduino Due) which functions as the parent. In total, the I2C bus required only 4 wires (3.3V, electric ground, clock, and data) to enable communication between the parent and the children. These four wires were integrated within a FFC to provide ease of use and a compact design. The overall thickness of the PCB including the height of the sensor chip and the thickness of the FFC connector has been designed to be 1.5mm.

B. Remote Center of Motion (RCM) Mechanism

To mimic the kinematics of the user's finger, a RCM mechanism was realized. A RCM mechanism can realize a pivot point outside of its mechanical structure. The mechanism is widely used in surgical devices or apparatus where a medical tool is to be rotated at an inaccessible or remote location such as inside the body of a patient. Zong et al. [19] illustrate the wide variety of ways in which RCM mechanisms can be used. RCMs also have been used for exoskeletons [20] and robot grippers [21]. The RCM mechanism in the current paper is embodied as a 6-bar linkage, as explained below. We use a RCM mechanism so that no revolute joint needs to be located next to the human finger. Revolute joints concentric with the human finger joints would have increased the width of the Exo-Glove, as they would have been thicker than the clamps, and would have also covered more of the skin of the user, overall decreasing the natural human-object interaction.

1) Human finger kinematics: The human finger consists of 3 joints and 4 revolute pairs. The three joints are designated as DIP (Distal Interphalangeal) joint, PIP (Proximal interphalangeal) joint and MCP (Metacarpal Interphalangeal) joint. The DIP and PIP joints have one degree of freedom respectively whereas the MCP joint is a two degree of freedom joint. In total the human finger has four degrees of freedoms.

2) Schematic representation of the RCM mechanism: Fig. 6 shows the schematic representation of the RCM mechanism. A 6-bar linkage embodies the RCM mechanism. The 6 links are oriented to form two parallelograms ABET and CDTF. In order to mimic the kinematics of the finger the remote center of motion is placed concentric to the center of rotation of the human finger joint as shown in the Fig. 6.

Angle 2 is fixed by adjusting link ED such that the imaginary line ET, which is colinear to link ED, coincides with the DIP joint. Similarly, angle 1 is fixed by adjusting link AF such that point T will be co-linear with link AF via an imaginary line FT. With both angles set, the lengths of link BE and CF are chosen such that BE||AF where BE=AT and CF||DT where CF=DE. Further, BE and CF intersect at point G such that, BG=AF and CG=DE. Finally, points A, B, C and D were connected with links AB and CD respectively. Thus, two parallelograms ABET and CDTF were formed intersecting at point G. When the user would flex the finger as shown in the Fig. 6, the fingertip tactile

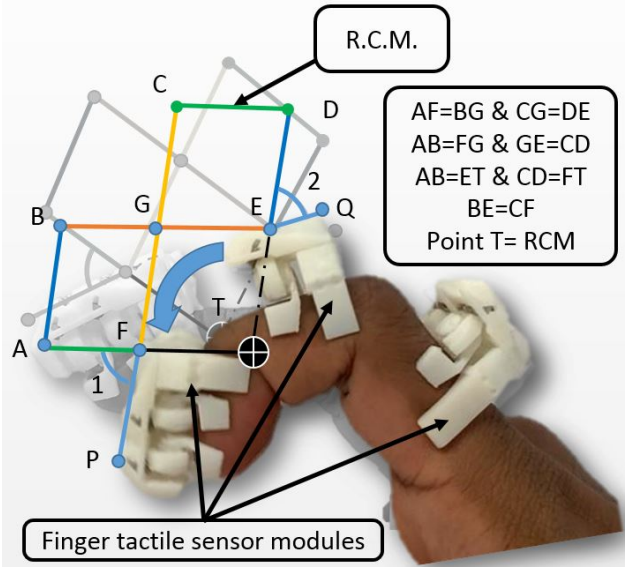

Fig. 6: RCM mechanism kinematics while flexing the finger

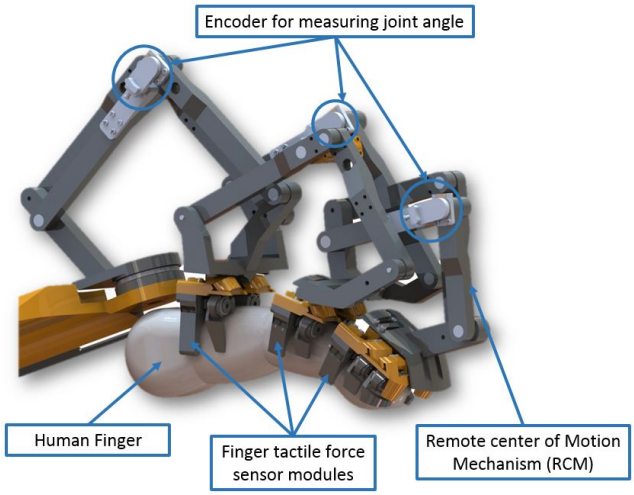

Fig. 7: 3D CAD design of Exo-Glove

sensor module along with link AF would rotate about point T which is concentric with the DIP joint. This would cause link BE to rotate about point E, following the geometry of the parallelogram (ABET). The intersecting point G causes the links CD and CF to displace, following the parallelogram (CDTF) geometry. Thus, the RCM mechanism ensures that the fingertip tactile sensor module rotates about point T while the middle tactile sensor module forms the mechanical frame of reference for the fingertip tactile sensor module.

In a similar manner, the links of the RCM mechanisms were designed for the PIP and the MCP joints. For the 4th revolute pair of the MCP a simple revolute joint was chosen. Thus, an entire mechanical linkage consisting of three RCM mechanisms and one revolute joint was designed. The Exo-Glove is illustrated in Fig.7. The Exo-Glove is worn with the help of elastic straps wrapped around the palm of the user forming a fixed frame of reference for

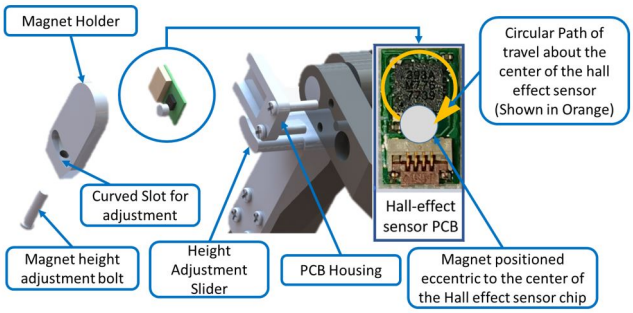

Fig. 8: Exploded view of Hall-effect based encoder

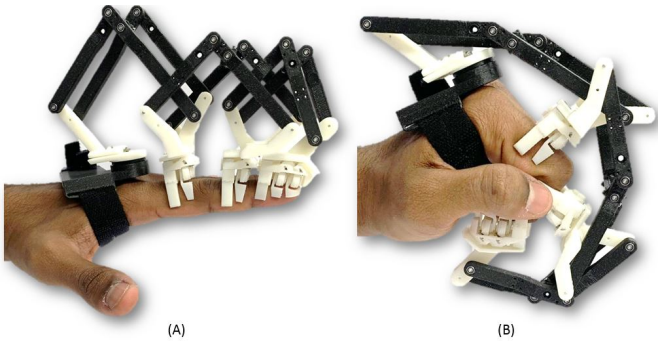

Fig. 9: A:Extension, B: Flexion

the entire Exo-Glove. The mechanical linkages of the Exo-Glove were manufactured with the help of an extrusion based Prusa 3D printer. The tactile sensor modules are attached to the mechanical linkages via 3D printed SLA adapters. The sensors were fastened to the adaptors with the help of the bolt and nut arrangement. The adapters formed the base links AF and DE respectively for each sensor module as shown in Fig. 6.

C. Joint Encoder

To measure the joint angles between the finger segments, the mechanical linkages are embedded with Hall-effect based encoders as shown in Fig. 7. The encoder uses the same Hall-effect sensor PCB comprising of the MLX90393 chip as shown in Fig. 8. The north pole of the magnet facing the sensor PCB is aligned eccentric to the center of the Hall-effect sensor chip as shown in the figure. The magnet is housed within a 3D printed magnet holder. The height of the magnet holder can be adjusted by loosening and fastening a bolt attached from the rear of the magnet holder and sliding the magnet holder up and down over a curved slot as also shown in the figure. The Hall-effect sensor PCB is then housed within a PCB housing fixed concentric to the center of the joint of the mechanical linkage. As shown in Fig. 7, three encoders were embedded into the mechanical joints of the Exo-Glove to measure the corresponding joint angles of the human finger joints (DIP, PIP, and MCP).

IV. Exo-Glove Evaluation

The Exo-Glove was 3D printed and assembled as shown in the Fig. 9 below. Velcro straps were used to rigidly mount the Exo-Glove on the palm of the user. The overall weight of the Exo-Glove was 30.96 grams.

In preliminary experiments with one subject we could validate that the subject was able to flex and extend his finger while wearing the Exo-Glove (the experiment is shown in Fig. 9). Moreover, the video accompanying the paper shows that the sensors do not detach from the finger during repeated flexion and extension. Furthermore, while wearing the Exo-Glove, the subject was able to grasp different objects, i.e. office tools such as cutters, pincers and some scholastic tools such as writing pens and markers. Fig. 10 illustrates some of the grasps. This is a first indication that the Exo-Glove could allow a natural human-object interaction. However,

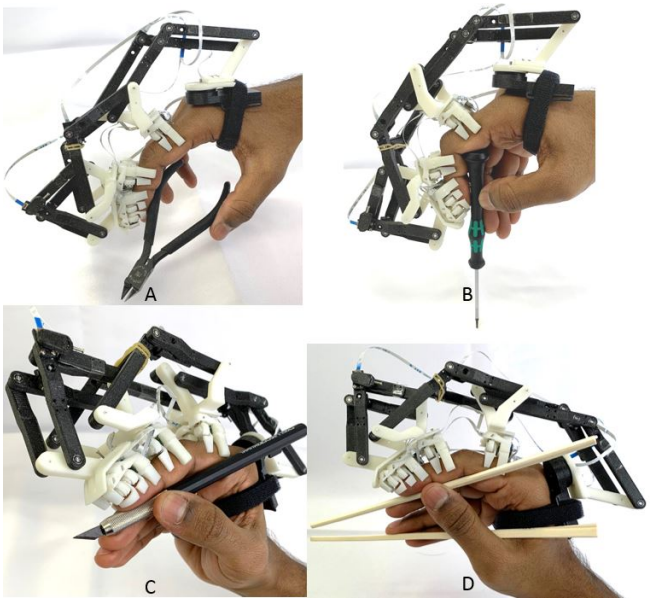

Fig. 10: Different Grasps

even though the Exo-Glove is lightweight, it is relatively large and the weight is located at a considerable distance to the finger. When the Exo-Glove is oriented horizontally (for example when the hand performs a handshake) it applies a considerable torque to the finger. This is a hindrance to the human, especially when wearing the Exo-Glove for extended periods of time. Moreover, the Exo-Glove is not appropriate for situations in which the human hand or finger needs to work in narrow spaces. Therefore, the form factor of the Exo-Glove limits the kind of tasks that can be studied with it.

A. Sensor Calibration

To evaluate the performance of the fingertip tactile sensor after introducing the mechanical frame of reference from the RCM mechanism, a calibration setup similar to the one previously presented in the paper [1] was used. The evaluation was made with and without the Exo-Glove. We used supervised learning to calibrate the finger tactile sensor as shown in the Fig. 11. An ATI Nano 17 6-axis F/T sensor was used as reference sensor of our calibration setup. When calibrating the finger tactile sensor, both reference sensor

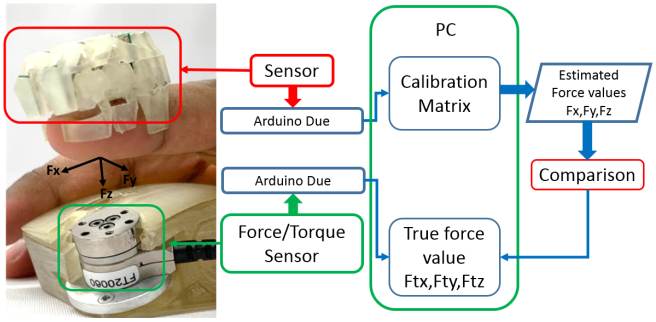

Fig. 11: Calibration Setup

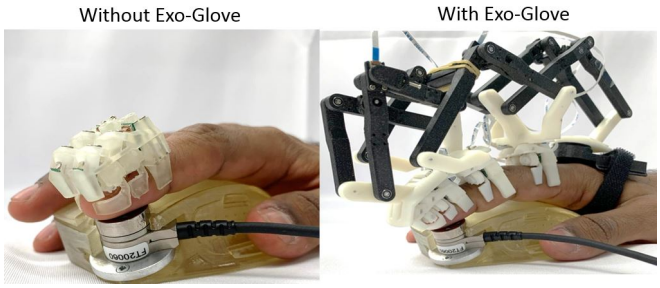

Fig. 12: Calibration Setup with and without the Exo-Glove

and finger tactile sensor data were recorded together. For both the stages (without Exo-Glove and with Exo-Glove as shown in Fig. 12) two sets of data samples were taken; calibration data for learning and test data for evaluation. Linear regression was used to derive the relationship between magnetic measurements and the force applied by the fingertip on the reference sensor. A linear model was used as it provided better results on independent test data than a quadratic model in our previous work [1]. The 6-axis force torque sensor was housed within an ergonomic palmrest. The palmrest was designed to rigidly mount the sensor and inherently prevent it from displacing due to the force applied by the fingertip. The shape of the palmrest was inspired by the shape of a computer mouse as shown in Fig. 12. The palm rest facilitated the user to apply forces with only the finger, as well as placing each subject's finger in the same position for all trials.

B. Calibration Procedure and Experiment

The calibration and evaluation were performed with 7 people. For calibrating the sensor for each person, the respective subject was asked to apply force for 20 seconds in each direction (-Z, +X, -X, +Y, -Y). The orientations of the axes are shown in Fig. 11. The subjects were asked to apply the maximum force in each direction which they could apply with ease. The subjects rested their palm on the computer-mouse-shaped support and were asked to apply forces only with their fingers. For evaluation, the subjects applied step-wise force in each direction, as shown in Fig. 13 and Fig. 14. The procedures for acquiring training and test data were the same as in our previous work, which describes the procedure in more detail [1]. According to preliminary experiments conducted in [1], most subjects were able to comfortably exert forces with their index finger in the range of +/- 2N in the X and Y direction and -4N in the Z direction. It was also realized that the sensor saturates for higher forces. Therefore, we set those forces as the range of forces also in the current paper.

C. Calibration and Test Procedure of Hall-effect Sensor based Encoder

This section describes the calibration and validation procedure of the Hall-effect based encoders embedded within the mechanical linkage of the RCM mechanism.

1) Calibration (Procedure to acquire training data): A human finger joint does not have a fixed center of rotation but the center of rotation shifts with the joint angle. Although it is difficult to locate the center of rotation of the human finger joint, the angle between two finger segments can be measured using a goniometer, shown in Fig. 15, and it is widely used by medical practitioners and physiotherapists. To calibrate the Exo-Glove, the subject was first asked to wear the Exo-Glove. The goniometer was then attached to his hand such that the baseplate of the goniometer aligned with the middle phalange with the help of a mechanical harness as shown in Fig. 15. The candidate was asked to rest his middle and distal phalanges on the surface of a table. The subject was asked to flex the PIP joint in increments of 5 degrees with the assistance of visual feedback from the goniometer. We visually checked the goniometer and noted down the actual joint angles that the subject achieved Raw magnetic data was recorded from the encoder corresponding to the PIP joint and a linear model was used to convert this raw data to angular measurements.

$$\theta = aX + bY + cZ \tag{1}$$

Here, θ is the calibrated angle measurement of the encoder output. X, Y and Z are the raw magnetic measurements from the Hall-effect sensor. a, b and c are the calibration parameters obtained with MATLAB using the Statistics and Machine Learning Toolbox. In future work we plan to employ more complex calibration functions, such as a sinusoidal one.

2) Validation (Procedure to acquire test data): To test the encoder corresponding to the PIP joint, the subject was asked to extend the PIP joint in 10-degree increments, starting from a fully flexed state.

V. Results

Figs. 13 and 14 show a representative example of the forces measured by the fingertip sensor, compared to the forces measured by the reference sensor, without and with the Exo-glove, respectively. In particular, the test results of one subject are shown. In the rightmost plot of Fig. 14 it appears that the z-axis measurement drifts, but such drift could not be observed in the results of other subjects. Instead we expect that this apparent drift is due to hysteresis, as the finger flesh tends to return only slowly to its original shape after having applied relatively high forces. Fig. 16 shows the average error of all 7 subjects of the forces predicted by the

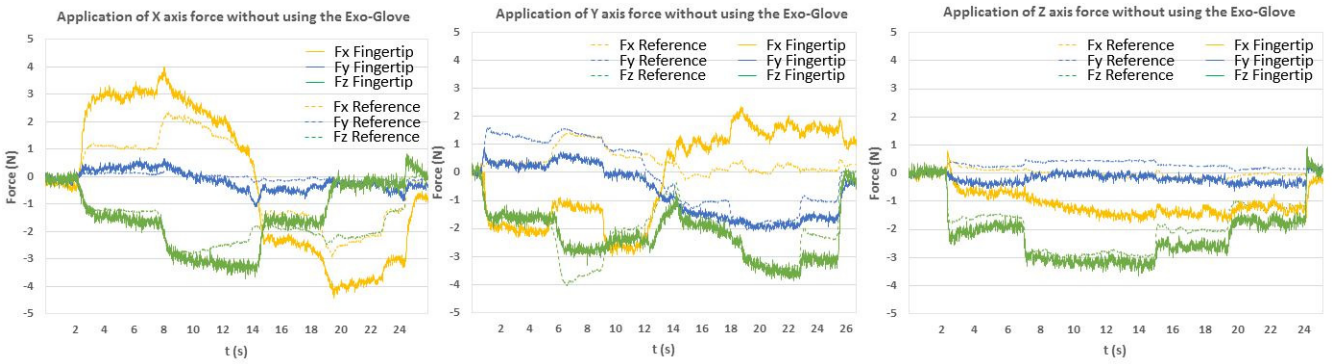

Fig. 13: Without Exo-Glove

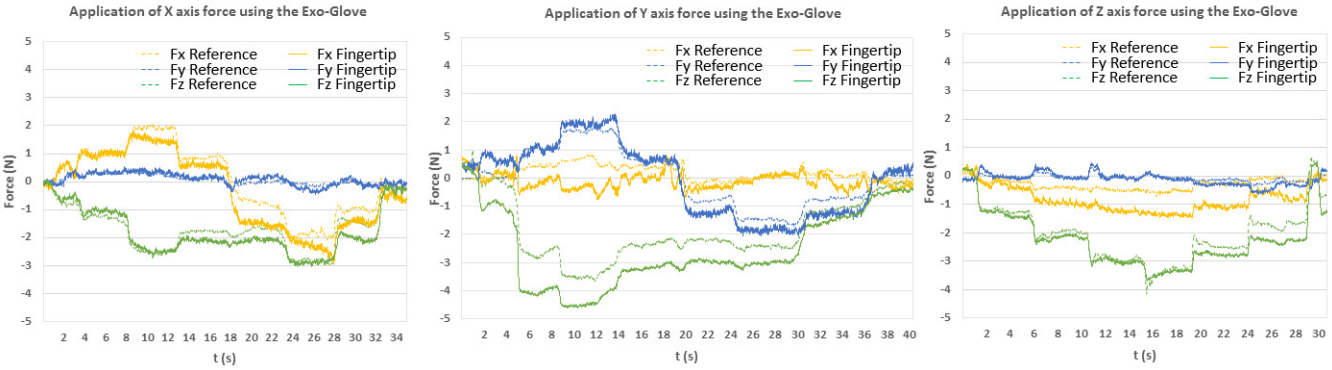

Fig. 14: With Exo-Glove

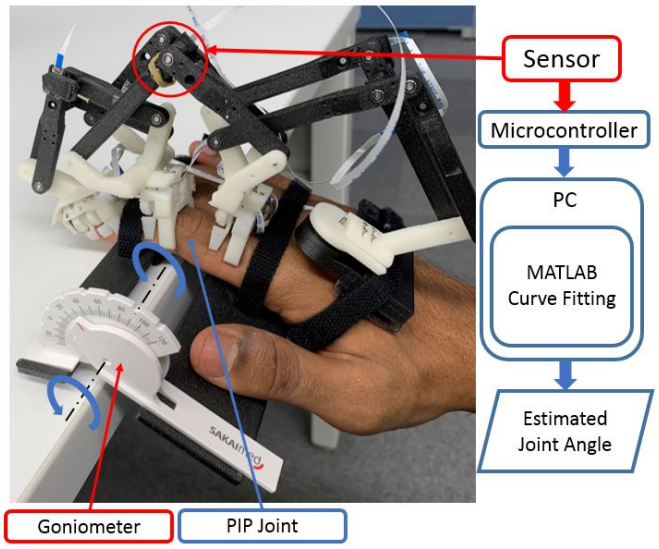

Fig. 15: Encoder Calibration and Experiment

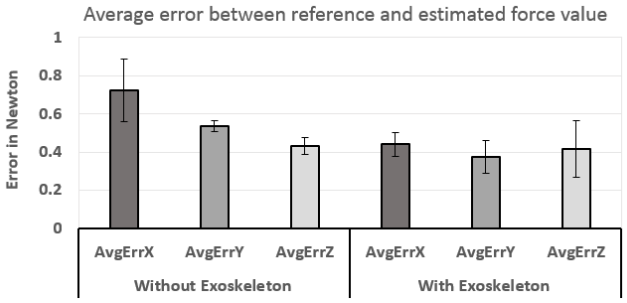

Fig. 16: Mean Error between reference force vector value and estimated force vector value. The standard deviation is also shown.

sensor without and with the Exo-Glove. By using the Exo-glove the error in Y axis reduces by about 300mN and the error in X axis reduces by about 160mN. The overall error (resultant force) reduces by about 310mN. The accuracy of the sensor can be seen in Table I and was calculated using equation (2).

$$Accuracy\% = 100 - \frac{|Force_{finger} - Force_{reference}|}{OverallForceRange} \times 100 \quad (2)$$

From Fig. 16 and Table I we can say that by using a dynamic frame of reference such as the Exo-glove, one can now measure the shear force more accurately.

Fig. 17 presents the results for the angular measurement. In particular, the test subject was asked to extend the PIP joint of his index finger in increments of 10 degrees. The blue line shows the result from our suggested angular sensor vs. the values from the goniometer. Overall, it was observed

TABLE I: Overall Accuracy With and Without Exo-Glove

Accuracy	x-axis	y-axis	z-axis
Without Exo-Glove	72.4%	85.3%	90.2%
With Exo-Glove	91%	91.7%	94%

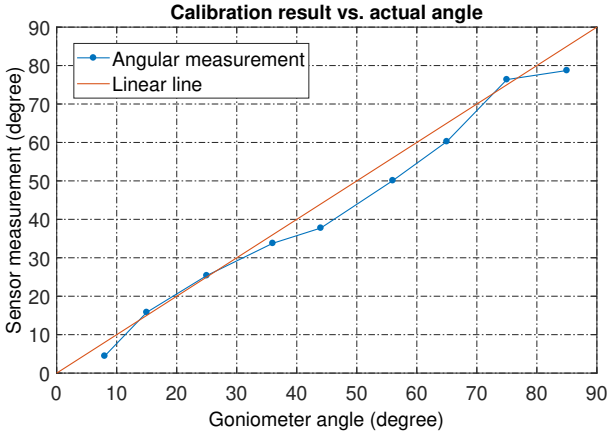

Fig. 17: Calibrated sensor (encoder) values vs. goniometer values

that a variation of $\pm$ 5^o was observed. The accuracy for the angular sensor was calculated as 96.10 $\pm$ 2.66% from the measurements presented in Fig. 17, using a range of 90^o.

VI. Conclusions and Future Work

This paper presented a sensor system for human fingers. The joint angles as well as the forces acting on the finger can be measured, without covering the skin that is contact with the object. Different grasps can be performed in an unobstructed fashion. Due to the improved reference frame that the Exo-Glove provides with the help of RCM joints, the accuracy of the force measurements could be improved compared to our previous work.

In future work, all fingers of the human hand should be covered with the Exo-Glove, and skill transfer from humans to robots will be investigated. In particular, our lab also has robot hands that are equipped with tactile sensors [22], which can be used to reproduce the joint trajectories and forces exerted by a human during various tasks.

References

[1] H. Kristanto, P. Sathe, A. Schmitz, C. Hsu, T. P. Tomo, S. Somlor, and S. Sugano, "Development of a 3-axis human fingertip tactile sensor based on distributed hall effect sensors," in *2019 IEEE-RAS 19th International Conference on Humanoid Robots (Humanoids)*, 2019.

[2] D. J. Beebe, D. D. Denton, R. G. Radwin, and J. G. Webster, "A silicon-based tactile sensor for finger-mounted applications," *IEEE Transactions on Biomedical Engineering*, vol. 45, no. 2, pp. 151–159, Feb. 1998.

[3] S. A. Mascaro and H. H. Asada, "Photoplethysmograph fingernail sensors for measuring finger forces without haptic obstruction," *IEEE Transactions on Robotics and Automation*, vol. 17, no. 5, pp. 698–708, Oct. 2001.

[4] ——, "Measurement of finger posture and three-axis fingertip touch force using fingernail sensors," *IEEE Transactions on Robotics and Automation*, vol. 20, no. 1, pp. 26–35, Feb. 2004.

[5] T. R. Grieve, J. M. Hollerbach, and S. A. Mascaro, "3-D Fingertip Touch Force Prediction Using Fingernail Imaging With Automated Calibration," *IEEE Transactions on Robotics*, vol. 31, no. 5, pp. 1116–1129, Oct. 2015.

[6] ——, "Force prediction by fingernail imaging using active appearance models," in *2013 World Haptics Conference (WHC)*, Apr. 2013, pp. 181–186.

[7] T. R. Grieve, C. E. Doyle, J. M. Hollerbach, and S. A. Mascaro, "Calibration of fingernail imaging for multidigit force measurement," in *2014 IEEE Haptics Symposium (HAPTICS)*, Feb. 2014, pp. 623–627.

[8] T. R. Grieve, J. M. Hollerbach, and S. A. Mascaro, "Fingernail image registration using Active Appearance Models," in *2013 IEEE International Conference on Robotics and Automation*, May 2013, pp. 3026–3033.

[9] E. R. Serina, C. Mote, and D. Rempel, "Force response of the fingertip pulp to repeated compression – effects of loading rate, loading angle and anthropometry," *Journal of Biomechanics*, vol. 30, no. 10, pp. 1035–1040, Oct. 1997.

[10] E. R. Serina, E. Mockensturm, C. D. Mote Jr., and D. Rempel, "A structural model of the forced compression of the fingertip pulp," *Journal of Biomechanics*, vol. 31, no. 7, pp. 639–646, Jul. 1998.

[11] Y. Matsuura, S. Okamoto, and Y. Yamada, "Estimation of Finger Pad Deformation Based on Skin Deformation Transferred to the Radial Side," in *Haptics: Neuroscience, Devices, Modeling, and Applications*, ser. Lecture Notes in Computer Science. Springer, Berlin, Heidelberg, Jun. 2014, pp. 313–319.

[12] A. G. Perez, G. Cirio, D. Lobo, F. Chinello, D. Prattichizzo, and M. A. Otaduy, "Efficient nonlinear skin simulation for multi-finger tactile rendering," in *2016 IEEE Haptics Symposium (HAPTICS)*, 2016, pp. 155–160.

[13] M. Nakatani, T. Kawasoe, K. Shiojima, K. Koketsu, S. Kinoshita, and J. Wada, "Wearable contact force sensor system based on fingerpad deformation," in *2011 IEEE World Haptics Conference*, Jun. 2011, pp. 323–328.

[14] A. Saito, W. Kuno, W. Kawai, N. Miyata, and Y. Sugiura, "Estimation of fingertip contact force by measuring skin deformation and posture with photo-reflective sensors," in *Proceedings of the 10th Augmented Human International Conference 2019*, ser. AH2019. New York, NY, USA: ACM, 2019, pp. 2:1–2:6.

[15] Y. Tanaka, D. P. Nguyen, T. Fukuda, and A. Sano, "Wearable skin vibration sensor using a PVDF film," in *2015 IEEE World Haptics Conference (WHC)*, Jun. 2015, pp. 146–151.

[16] E. Battaglia, M. Bianchi, A. Altobelli, G. Grioli, M. G. Catalano, A. Serio, M. Santello, and A. Bicchi, "Thimblesense: A fingertip-wearable tactile sensor for grasp analysis," *IEEE Transactions on Haptics*, vol. 9, no. 1, pp. 121–133, Jan 2016.

[17] E. Battaglia, M. G. Catalano, G. Grioli, M. Bianchi, and A. Bicchi, "Exosense: Measuring manipulation in a wearable manner," in *2018 IEEE International Conference on Robotics and Automation (ICRA)*, 2018, pp. 2774–2781.

[18] M. Bianchi, R. Haschke, G. Büscher, S. Ciotti, N. Carbonaro, and A. Tognetti, "A multi-modal sensing glove for human manual-interaction studies," *Electronics*, vol. 5, no. 3, 2016. [Online]. Available: https://www.mdpi.com/2079-9292/5/3/42

[19] G. Zong, X. Pei, J. Yu, and S. Bi, "Classification and type synthesis of 1-dof remote center of motion mechanisms," *Mechanism and Machine Theory*, vol. 43, no. 12, pp. 1585 – 1595, 2008.

[20] M. Fontana, S. Fabio, S. Marcheschi, and M. Bergamasco, "Haptic hand exoskeleton for precision grasp simulation," *Journal of Mechanisms and Robotics*, vol. 5, no. 4, 2013.

[21] C. HSU, A. SCHMITZ, G. KHULLAR, H. KRISTANTO, Z. WANG, P. SATHE, and S. SUGANO, "Implementation of a remote center of motion robot finger with tactile sensors in the joints," in *2019 IEEE International Conference on Robotics and Biomimetics (ROBIO)*, Dec 2019, pp. 247–252.

[22] T. P. Tomo, A. Schmitz, W. K. Wong, H. Kristanto, S. Somlor, J. Hwang, L. Jamone, and S. Sugano, "Covering a Robot Fingertip With uSkin: A Soft Electronic Skin With Distributed 3-Axis Force Sensitive Elements for Robot Hands," *IEEE Robotics and Automation Letters*, vol. 3, no. 1, pp. 124–131, Jan. 2018.